Title: Glycine decarboxylase deficiency impairs motor behaviour in zebrafish rescued by counterbalancing glycine synaptic level.

Raphaëlle Riché[1], Meijiang Liao[1], Izabella A. Pena[2], Kit-Yi Leung[3], Nathalie Lepage[2], Nicolas D.E. Greene[3], Kyriakie Sarafoglou[4], Lisa A. Schimmenti[5], Pierre Drapeau[1,6] and Éric Samarut[1,6*].

1-Research Center of the University of Montreal Hospital Center (CRCHUM), Department of Neurosciences, Université de Montréal, Montréal, QC, Canada.

2- Children's Hospital of Eastern Ontario Research Institute and Department of Pediatrics, Faculty of Medicine, University of Ottawa, Ontario K1H 8L1, Canada

3- Developmental Biology & Cancer Programme, UCL Great Ormond Street Institute of Child Health, University College London, London WC1N 1EH, UK

4- Division of Pediatric Endocrinology, Department of Pediatrics, University of Minnesota, Minneapolis, Minnesota, USA

5- Mayo Clinic College of Medicine, Department of Otorhinolaryngology, Rochester, MN, United States; Mayo Clinic College of Medicine, Department of Pediatrics, Rochester, MN, United States; Mayo Clinic College of Medicine, Department of Clinical Genomics, Rochester, MN, United States.

6-DanioDesign Inc., Montréal, QC, Canada.

corresponding author: eric.samarut@umontreal.ca

The authors have declared that no conflict of interest exists.

Graphical Abstract

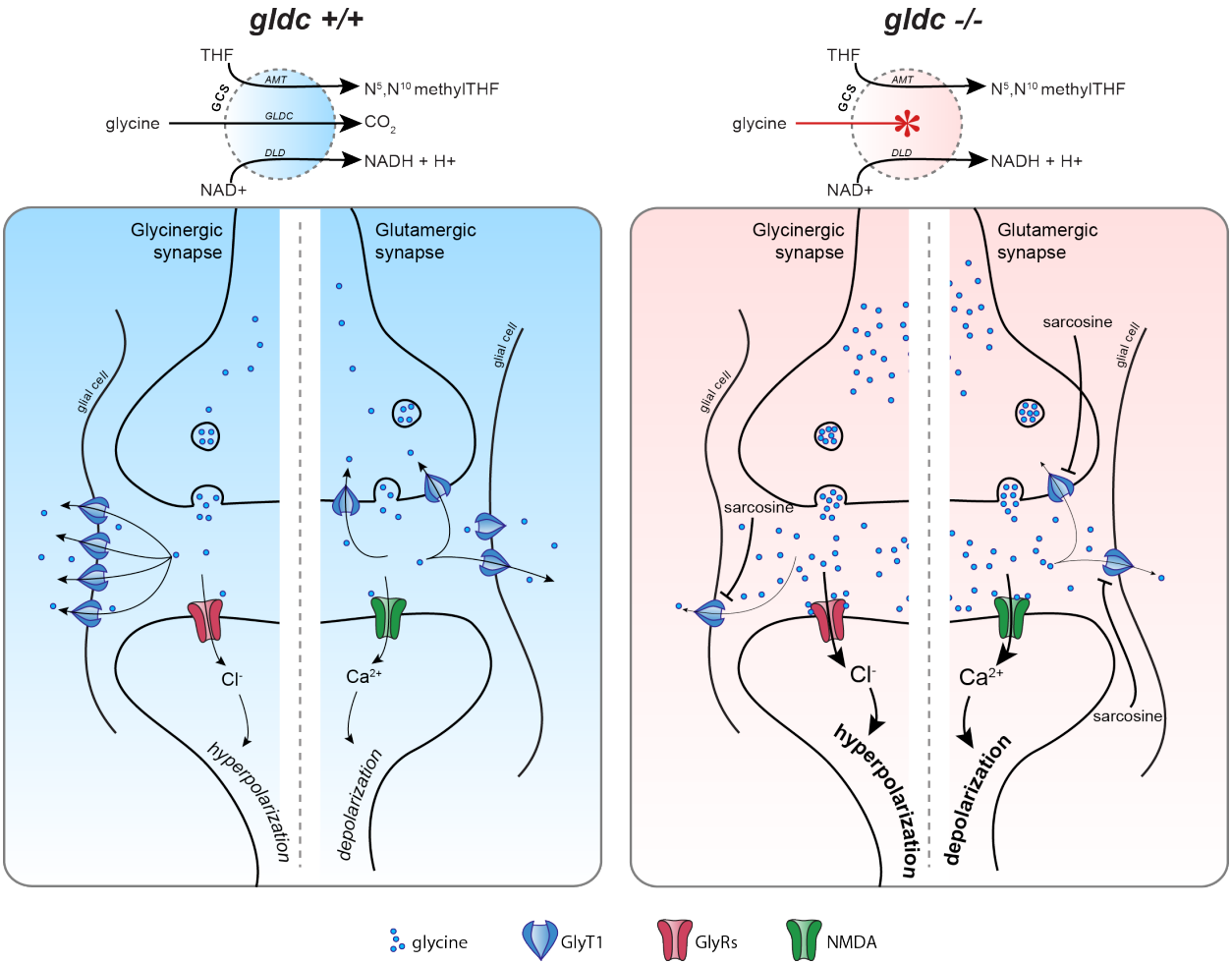

Abstract

Glycine encephalopathy (GE) or Non-Ketotic Hyperglycinemia (NKH), is a rare recessive genetic disease caused by defective glycine cleavage and characterized by an increased accumulation of glycine in all tissues. Here, based on new case-reports of *GLDC* loss-of-function mutations in GE patients, we aimed at generating a zebrafish model of severe GE in order to unravel the molecular substratum of the disease._Using CRISPR/CAS9, we knocked-out *gldc* gene and showed that *-/-* fish recapitulate GE on a molecular level and depict a motor phenotype reminiscent of severe GE symptoms. The molecular characterization of *gldc -/-* mutants showed a broad metabolic disturbance affecting amino acids and neurotransmitters other than glycine, with lactic acidosis at stages preceding death. Although a transient imbalance was found in cell proliferation in the brain of *gldc -/-*, the main brain networks are not affected thus suggesting that GE pathogenicity is mainly due to metabolic defects._We confirmed that the *gldc -/-* hypotonic phenotype is due to NMDA and glycine receptors overactivation, and demonstrated that *gldc*-/- larvae depict an exacerbated hyperglycinemia at these synapses. Remarkably, we were able to rescue the motor dysfunction of *gldc*-/- larve by counterbalancing pharmacologically or genetically the level of glycine at the synapse.

Introduction

Glycine encephalopathy (GE), also known as nonketotic hyperglycinemia (MIM 605899), is a rare genetic defect in glycine metabolism characterized by a considerable accumulation of glycine in all tissues, especially in the central nervous system (1-4). GE has an autosomal recessive inheritance pattern and is classically caused by mutations in proteins of the glycine cleavage system composed of a glycine decarboxylase (GLDC), an aminomethyltransferase (AMT), a hydrogen carrier protein (GCSH), and a dihydrolipoamide dehydrogenase (DLD) (4, 5). All four subunits are encoded by distinct genes and *GLDC* is mutated in 72% of the GE cases(2).

The symptoms of GE are commonly first observed during the neonatal period and are very heterogeneous among the patients, depending on the pathogenicity of the mutation (5, 6). In severe GE, the neonates present severe hypotonia, myoclonic jerks, lethargy and apnea due to respiratory depression, which often causes death within the first week of life. The patients with severe GE surviving the neonatal period make no developmental progress and show spasticity, intractable seizures and hypotonia. Individuals with attenuated GE often survive the neonatal period but show treatable seizures, spasticity, chorea and variable developmental delay that often leads to intellectual disability (5, 6).

The treatments available for GE patients are primarily used to alleviate the symptoms but do not resolve the underlying metabolic defects. Indeed, dextromethorphan, an NMDA receptor antagonist, is used to diminish the seizures, and sodium benzoate helps reduce glycine levels by elimination through the urine. Unfortunately, even when combined these treatments fail to improve the outcome of many GE patients (6). However, although the clinical research

done on human patients has helped identify the genetic causes of the disease and characterize the spectrum of symptoms, it has not elucidated the molecular basis of GE.

A few research efforts have been made to model the disease. In mouse, a loss-of-function gene-trap allele and a dominant-negative model of *gldc* that show features of GE, such as early lethality, increased glycine, and hydrocephalus, were generated (7, 8). A zebrafish model was described in which the hyperglycinemia is restricted to the brain, but it cannot be used to study the classical form of the disease (9). These models help understand aspects of GE, but did not focus on characterizing the pathogenic mechanisms underlying the disease. As a result, this highlights the necessity of generating an accurate and reliable animal model of GE, more amenable to metabolic analyses and high throughput drug screens.

Here we report two new cases of GE patients carrying loss-of-function mutations in one or both *GLDC* alleles. At this juncture, we generated a zebrafish model of GE (*gldc-/-)* depicting high level of glycine and displaying motor abnormalities and premature death, thus resembling the fatal outcome of severe forms of GE. Next, we performed unbiased high-throughput proteomics and transcriptomics analysis and showed that *gldc* loss-of-function induces broad metabolic defects. We also confirmed synaptic glycine-signaling abnormalities and remarkably were able to rescue the hypotonic phenotype of *gldc -/-* larvae by counterbalancing the hyperglycinemia at the synapse.

Results

Two case-reports of GE associated with mono-allelic or bi-allelic LOF-mutations in GLDC

The first patient we examined was a deceased female infant born at 39 week gestational age. Pregnancy was uncomplicated and she was delivered vaginally with Apgar scores of 8 at one minute and 9 at five minutes. She was discharged from the nursery at 2 days of life. At 4 days of life she became lethargic with poor feeding and was admitted again. Her physical examination was significant for respiratory failure requiring intubation, diffuse hypotonia, absent deep tendon reflexes, withdrawal to painful stimuli, rhythmic hiccupping and myoclonic movements of the right upper extremity. MRI on day 4 of life revealed a small but completely formed corpus callosum with a mild delay in myelination and a slightly lower volume of cerebral white matter. EEG revealed burst suppression pattern. Her seizures were treated with phenobarbital and ativan, but were relatively refractory to medication. Additional testing revealed an elevated plasma glycine level of 125 umol/dL (0-57) and elevated glycine CSF of 33.8 umol/dL (0.2-2.0). The CSF/plasma glycine ratio of 0.27 (pathognomonic ratio >0.08) was diagnostic of GE (or nonketotic hyperglycinemia). Given the grave prognosis of this disease, the infant's family decided to withdraw life-sustaining treatment on day 10 of life. Newborn screening was negative and chromosomal studies were pending at the time of death. Molecular testing revealed two variants in the *GLCD* gene: c.1153 C>T (p.Q385X) and c.941 ins16nt fs (Figure 1).

The second patient was a 50-year-old gentleman who presented initially to adult neurology for a movement disorder. He was non-verbal, had limited facial expression, drooled, and had a constant tremor. He was unable to walk unassisted and required caretakers to assist with personal tasks such as feeding and toileting. He had a history of myoclonic jerks and was treated with valproic acid. Clinical evaluation identified a mild elevation of glycine. Genetic

testing identified two variants in *GLCD* c.1054delA(p.Thr352fster65) and c.1705C>T(p.Ala569Thr) (NM00170.2, Figure 1) and paternal testing supported that the variants were in trans. Although the first allele carrying a nonsense mutation is pathogenic, the second one with a missense mutation has been recently reported as non pathogenic with a residual enzymatic activity of about 70% (10). After the diagnosis, valproic acid was promptly discontinued and the patient was started on dextromethoraphan and sodium benzoate. Glycine levels fell into the normal range and the patient had improved mobility, resolution of constant tremors, stopped drooling, and was able to feed himself. However, his general quality of life was still severely impaired since he needs daily assistance.

These two cases demonstrate the clinical heterogeneity of GE and are consistent with previous study linking the severity of the disease with the residual GLDC enzymatic activity of different missense mutations (11).

Zebrafish gldc is expressed in the CNS and its loss-of-function induces glycine accumulation

We started by examining the *gldc* sequence and its expression in zebrafish embryos. In contrast to the common gene duplication in teleost fish, a single copy of the *gldc* gene can be found in the zebrafish genome (ENSDAR00000035120) and it shows more than 60% overall amino acid identity with the human protein. We also assessed the expression pattern of *gldc* uring zebrafish development by *in situ* hybridization from 8 hours post-fertilization (hpf) to 42 hpf. *Gldc* is broadly expressed in the nervous system until 32 hpf, and at 42 hpf its expression is in specific brain regions (Figure 2A). Interestingly, we observed that the expression become restricted to the midbrain/hindbrain boundary and the commissural regions of the brain from 3

dpf. From 4 dpf, *gldc* transcript starts to be strongly expressed in the liver, the intestine and the gut. This expression persists at 5 and 6 dpf with only a weak expression in the brain.

The significant level of identity between human and zebrafish GLDC and its strong expression in the embryonic CNS suggest a robust evolutionary conservation of GLDC function, thus supporting the pertinence of a *gldc* knock-out zebrafish to model the human disease.

In designing gRNAs for the CRISPR/CAS9-mediated mutagenesis, we targeted the beginning of the glycine cleavage domain with the aim of reproducing a pathogenic loss-of-function mutation. We selected a founder transmitting a 5 nucleotide deletion and 3 nucleotide mismatches early in the glycine cleavage domain, creating a stop codon at the 189th amino acid (Figure 2B-C). Using the high-resolution melting (HRM) analysis (12), we could easily identify all three genotypes (*+/+, -/+,* -/-) (Figure 2B). We confirmed *gldc* knock-out by RT-qPCR and showed that *-/-* embryos have reduced levels of *gldc* expression compared to their siblings, as seen in patients (13). More importantly, Liquid Chromatography – Mass Spectrometry (LC-MS) analysis of glycine levels in whole 7 dpf larvae supported the loss-of-function nature of the mutation, since *gldc -/-* larvae display 4 times more accumulated glycine than their siblings (Figure 2D). Altogether, these results show that our newly generated *gldc*-KO line recapitulates the main molecular hallmarks of GE.

Gldc -/- larvae die prematurely and depict GE-reminiscent motor phenotypes

While most of the *gldc +/+* and *-/+* larvae survived for the first 10 days post fertilization, all the *gldc -/-* larvae died between 7 and 9 dpf (Figure 3A). After measuring the body length, eye size and inter-eye distance of -/- larvae compared to their siblings, we did not notice any

morphological abnormalities of the mutant larvae (Figure 3B). However, *gldc -/-* larvae from 6 dpf depict an evident hyperpigmentation, which is practical to easily separate them from the siblings (Figure 3C). This hyperpigmentation phenotype segregates with the mutant alleles of *gldc* through multiple generations of fish, thus suggesting that, although unexpected, it is specific to *gldc* loss-of-function. Although no major morphological differences was observed, we performed transverse sections of different regions of the larval brain (forebrain, midbrain, hindbrain and anterior spinal cord) and we did not notice any obvious morphological difference between gldc+/+ and -/- at 7 dpf (Figure 3D).

Since the GE patients show early motor symptoms such as hypotonia and lethargy, we analyzed the larval motor function of the *gldc* mutants. Spontaneous coiling is the first motor output in zebrafish embryos occurring between 17-21 hpf and consisting of frequent un-evoked movements of the tail in the chorion (14). Analysis of this motor behavior indicated a decrease in coiling frequency of *gldc -/-* embryos compared to their siblings (1.46 ± 0.31 n=14, 12.81 ± 2.73 n=11; Figure 3E). At the larval stage, we assayed the swimming activity of *gldc* mutants by recording the total distance swam over one hour and we noticed a reduction of swimming activity in *gldc -/-* larvae at 7 dpf (650.6mm ± 138.4 n=23, 1646mm ± 332.1 n=10; Figure 3F). Of note is that this reduced swimming behavior starts at 4 dpf and is more and more evident with age.

Hypotonia and lethargy are respectively defined as a state of low muscle tone and a lack of vigor. Thus we tracked the path swam by gldc-/- larvae after applying a circular water current, as well as the time needed to immobilize in the dish (e.g. stabilize their position). While the siblings can actively swim against the water current in order to maintain their position, *gldc*

-/- mutants were unable to fight against it and to stabilize their position. As a result, they were passively carried through the dish by the water current in a lethargic and hypotonic fashion (Figure 3G). Consistently, the time to stabilize their position after applying water current is significantly increased compared to their siblings (Figure 3H). Furthermore, we noticed an anomaly in the swimming balance of *gldc -/-* larvae. Indeed, we noticed that while the siblings are exploring their tank by swimming throughout it, most of the *gldc -/-* larvae float at the surface, unable to explore their environment, indicating a swimming balance impairment (Figure 3I-J(Figure 3C).). Of note is that although seizures are often reported in GE patients, electrophysiology recordings from larval brains did not detect any electrical discharge in gldc-/- (data not shown). Taken together these results show that the *gldc -/-* mutants display motor phenotypes reminiscent of GE symptoms in human patients, such as early lethality, hypotonia, and lethargy.

Metabolomics analysis indicates broad metabolic perturbations in gldc -/- larvae.

After characterizing the disease-related phenotype of *gldc -/-* mutants, we sought to describe the molecular mechanisms involved in pathogenicity. Since glycine acts as an essential amino-acid as well as a neurotransmitter in the CNS, we conducted a broad assay of metabolites by LC-MS in order to titrate the level of all proteinogenic and the main non-proteinogenic amino acids, as well as the main neurotransmitters. Interestingly, we found that extracts from *gldc -/-* larvae showed a significant increase in many amino acids other than glycine, such as sarcosine, proline, valine, cystathionine, leucine, and arginine (Figure 4A). Moreover, we found that *gldc -/-* larvae depicted a significant reduction in the levels of GABA

and glutamate compared to *gldc +/+* (Figure 4B) whereas dopamine and serotonin levels were not significantly affected. Likewise, this suggests that *gldc*-KO impairs the metabolism of amino-acid/neurotransmitters other than glycine. We next sought to determine if these changes are the result of an accumulation over time or if they are directly linked with GLDC-KO. Thus, we performed the same LC-MS analysis at 2 dpf and noticed that only sarcosine and glycine were already significantly increases in gldc-/- (Figure S1). This suggest that the increased level of proline, valine, cystathionine, leucine and arginine arise with time. We also found that at this early stage, methionine is significantly decreases in mutant embryos although this change does not persist until 7 dpf.

The GCS is also involved in folate one carbon metabolism (FOCM) since by degrading glycine, *gldc* donates one carbon units to this metabolic cycle(7, 15, 16). Thus, we examined the levels of FOCM-related metabolites in *gldc -/-* larvae in order to check whether an imbalance in this metabolism is consistently observed in our fish model. However, LC-MS titration of different folate-related metabolites did not reveal any defect of the FOCM in *gldc -/-* larvae as compared to *gldc +/+* (Figure 4C). We also noted that THF makes up approximately 60% of total folate in zebrafish larvae. This is markedly different to mammalian (mouse and human) tissue or E.coli in which 5-methyl THF or formyl-THF are abundant(15).

Finally, we also investigated the levels of lactate, since lactic acidosis is common in a number of metabolic inborn errors and has been reported in patients with GE (17-19). We found that the levels of lactate in *gldc -/-* mutants were significantly increased at 7 dpf. Interestingly, there was no difference in the levels of lactate in *gldc -/-* and *+/+* at 2 dpf,

suggesting that there is a progressive accumulation of lactate that leads to lactic acidosis at 7 dpf, whereas the levels of glycine are already increased at 2 dpf in *gldc -/-* (Figure 3D).

Altogether, these results demonstrate that *gldc* loss-of-function induces previously unknown broad metabolic perturbations.

Transcriptomics analysis reveals differences in the expression of cell cycle, proliferation, and metabolism-related genes in the gldc -/- mutants

In the continuity of the unbiased metabolomics analysis in the *gldc -/-* mutants, we carried out a whole transcriptome analysis by deep-sequencing of RNAs extracted from 7 dpf *gldc -/-* and *+/+* larvae. There were 408 differentially expressed genes in *gldc -/-* versus *gldc +/+* larvae, of which 153 were up- and 255 were downregulated (Figure 5A). Using gene clustering and pathway analysis from the list of significant differentially expressed genes, we identified multiple pathways whose gene expression was affected. As expected, multiple genes involved in general metabolism are mis-regulated in *gldc -/-* larvae. As an example, the amino acid transporter *slc6a19* was downregulated in *gldc -/-* (FC: -2.14, p=3.61E-16, and its mutation in human causes a metabolic disorder of neutral amino acid transport, Hartnup disease (Figure 5B) (20). Unexpectedly, only few brain-specific genes were found differentially expressed. However, one of them, glycine transporter 1 (*slc6a9*), was down-regulated (FC: -1.61, p=1.65E-08) in *gldc*-/- compared to +/+, and is relevant in the context of a neurological disorder like GE.

In addition, genes involved in cell adhesion and the extracellular matrix (ECM), such as integrin beta 4 (FC: -1.5, p=6.18E-05) and laminin 3 (FC: -1.7, p=1.29E-05), were found downregulated in *gldc -/-* mutants. More interestingly, many genes involved in the cell cycle

(e.g. *gadd45ba*; FC: 1.72, p=3.39E-07, as well as known oncogenes (e.g. *c-fos* and *myc-b;* FC: 1.9, p=1.89E-07 and FC: 1.55, p=1.03E-07) and tumor suppressor genes (*bcl6a*; - FC: 1.45, p=1.03E-07) were mis-regulated in *gldc -/-* compared to *gldc +/+* larvae.

Altogether, these transcriptomic data suggest that the majority of genes whose expression is affected by GLDC-KO are related to metabolism and that, surprisingly, no major transcriptomic changes occur in the CNS. Moreover, these data pointed out that cell-cycle homeostasis may be perturbed in *gldc -/-* larvae suggesting that cell proliferation may be affected in *gldc -/-* mutants.

The main brain networks are not affected by gldc-KO despite a transient decrease of proliferation in gldc -/- brain

The imbalance in the expression of proliferation-related genes observed in *gldc -/-* mutants from the RNAseq analysis led us to investigate the proliferation homeostasis in the brain throughout neurodevelopment. Moreover, a decreased proliferation at embryonic stages has been reported in a mouse model of *GLDC*-KO (7). Thus, we performed immunohistochemistry (IHC) at different developmental time points (1, 3 and 7 dpf) using an antibody against the phosphorylated form of Histone 3 (pH3), which marks cells undergoing mitosis. Interestingly, this assay revealed a significant decrease in cellular proliferation in the brain of *gldc -/-* mutants at 1 and 3 dpf (Figure 6A and 6I). However, this slight decrease in proliferation does not sustain until later stages, since no difference is observed at 7 dpf between *gldc -/-* and *+/+* larvae (Figure 6I).

Since a difference in proliferation homeostasis at early stages of neurodevelopment may have an impact on the content of specific neural cell populations, we sought to investigate whether the major cell populations and/or structures of the brain neuronal networks were affected. First, we checked the general morphology of neuronal fibers in the brain of *gldc -/-* larvae compared to their siblings by immunolabelling acetylated tubulin (ac-Tub). No difference in the labeling of axonal tracks in the brain of *gldc -/-* and *+/+* was observable at 24 hpf, nor later stages (4 dpf) (Figure 6B). Then, we aimed at checking the structure and neural content of (i) the GABAergic network using the [dlx5-6:GFP] transgenic line (Figure 6C) (21), (ii) glutamatergic network using the [vglut:RFP] transgenic line (Figure 6D) (22), (iii) the dopamine network through immunolabelling against tyrosine hydroxylase (TH) (Figure 6E), as well as (iv) the cerebellum through immunolabelling against paravalbumin 7 (PAV7, labeling Purkinje cells) and vglut1 (labeling granule cells) (Figure 6F and 6G). When comparing the cell content and/or immunolabeled morphology of these neuronal networks at different time points (3, 5 and 7 dpf), we were unable to observe any differences in any of these brain network markers between *gldc -/-* to *+/+* brains. Finally, we also examined the branchiomotor neuron population using the [islet1:GFP] transgenic line as it is a sensitive measure of neural tube anormalities and found no aberrant development or migration of the trigeminal, facial and vagal motorneurons at 3 dpf *gldc -/-* mutants (Figure 6H) (22). These results indicate that the transient proliferation deficit observed at 3 dpf in *gldc -/-* does not lead to any major morphological defect in other brain networks. Thus, it is likely to solely reflect a transient difference in the proliferating rate of neural progenitors that has no aftermath on brain neural content and therefore no specific relevance to the motor phenotype.

Genetically and pharmacologically counteracting the exacerbated hyperglycinemia at the synapse rescues the motor phenotype of gldc -/-

Since our previous results suggest that GLDC-KO is not affecting neural networks, we hypothesized that *gldc -/-* phenotype may be mainly due to metabolic defects, as described above. As a neurotransmitter, glycine is involved in synaptic signaling through binding to glycine receptors at inhibitory synapses and to NMDA receptors at excitatory synapses. Thus, we wondered whether the hyperglycinemia observed in *gldc -/-* larvae was affecting both inhibitory and excitatory synaptic transmission. To test this, we performed a pharmacological assay treating *gldc* embryos with either a glycine receptor antagonist (strychnine) or an NMDA receptor antagonist (dextromethorphan). Overnight treatment with a low dose of strychnine, a dose not affecting WT larval behavior, rescued significantly the hypotonic swimming phenotype of 7 dpf *gldc -/-* larvae (Figure 7A). Moreover, acute treatment with dextromethorphan did not significantly rescue the early motor deficiency of *gldc -/-* embryos at 21 hpf, but a daily exposure rescue the swimming defect at 7 dpf (Figure 7B and C). These results show that the hyperglycinemia is indeed over-activating both glycine receptors and NMDA receptors throughout the brain, which contribute to the GE-related hypotonic motor phenotype.

Then, we hypothesized that diminishing the hyperglycinemia at the synapse by overexpressing GlyT1 (a glycine transporter clearing glycine from the synaptic cleft) in *gldc -/-* embryos may improve their motor deficits. To test this assumption, we cloned the *GlyT1* cDNA and *in vitro* synthesized its mRNA in order to inject it in the first cell of *gldc* zebrafish embryos. We co-injected it with a GFP-encoding mRNA (as a positive readout) to allow us to select the

GFP-positive embryo that overexpress GlyT1 ubiquitously in the embryo for up to 48 hpf. Interestingly, overexpression of GlyT1 in *gldc -/-* embryo was sufficient to completely rescue their early motor defect back to the level of their siblings (Figure 2D).

Altogether, these results confirm that the hyperglycinemia of *gldc -/-* larvae is affecting normal glycinergic and NMDA signaling. Remarkably, counterbalancing this local hyperglycinemia at the synapse through the overexpression of GlyT1 completely rescues the motor phenotype of *gldc -/-* embryos (Figure 7E).

Discussion

In this work, we described two new cases of severe and mild GE and generated a zebrafish model of GE by knocking-out *gldc* using CRISPR/CAS9, with the goal of characterizing the molecular mechanisms underlying GE. After showing the reminiscence of the gldc-/- phenotype with the symptoms of severe GE patients, we sought for unbiased changes in the metabolome and transcriptome, and our analysis revealed unexpected imbalances in the metabolism of amino acids and neurotransmitters other than glycine. Moreover, we found that gldc -/-mutants display lactic acidosis preceding their death. They do not show obvious abnormalities in the folate profile. Given the cell-type specific expression of gldc at the 7dpf it is possible that defect in 1C supply is subtle in whole embryo samples. A key output of FOCM is nucleotide biosynthesis and we find cell that proliferation in the brain is slowed down during development, leading to a transient decrease in the number of dividing cells at 1 and 3 dpf. This is consistent with finding of diminished cell prolliferation in the neuroepithelium of Gldc mutant embryos in mouse(7). However, this is not associated with any gross morphological anomaly in

the main brain structures or neuronal networks of *gldc -/-*, suggesting that this transient reduction of proliferation may be the consequence of metabolic perturbation, without having direct consequences on the motor phenotype. Finally, we confirmed that the hypotonic motor phenotype of *gldc -/-* mutants is mainly due to the overactivation of NMDA and glycine receptors by glycine at the synapse. Very interestingly, we showed that this hyperglycinemia at the synapse can be recovered by pharmacologically antagonizing these receptors, as well as by genetically increasing the expression of glycine transporter 1.

Interestingly, our findings suggest that there is an exacerbated hyperglycinemia at the synapse of *gldc -/-* mutants. Indeed, rather than compensating for the excess of glycine at the synapse, we found that some of the metabolic and transcriptomic changes induced by GLDC-KO could worsen the level of glycine in the synaptic cleft. In fact, GlyT1 expression is significantly decreased in *gldc -/-* compared to their siblings, suggesting that the clearance of glycine from the cleft may be slowed. Moreover, our metabolomics analysis revealed a significant increase of sarcosine in *gldc -/-* larvae, a non-proteogenic amino acid known to be a potent antagonist of GlyT1 activity. Indeed, sarcosine has raised a significant therapeutic interest in the recent years as a potential treatment for schizophrenia by increasing glycinergic response in the brain of patients (23). Moreover, the level of sarcosine is already significantly elevated at 2 dpf in gldc-/- embryo suggesting that this increase may be the result of a more direct effect of GLDC loss-of-function than the other changes in amino acid level that are accumulating over time. As a result, dampening the increase in the level of sarcosine from early stages may be an interesting experiment to test the relevance to target sarcosine therapeutically. Altogether, our findings highlight the fact that the elevated glycine level at the synapse may not be solely due to a

347 defect of glycine degradation, but also to other synergic changes that may be good candidates
348 as therapeutic targets (Figure 7E).

349 Consistent with the excess of glycine at the synapse, we showed that the overexpression
350 of GlyT1 in the embryo was sufficient to fully rescue their motor condition. This is of prime
351 interest for further therapeutic strategies targeting GlyT1 activity. A significant interest has
352 been raised to develop potent antagonists of glycine transporters for the treatment of
353 schizophrenia, increasing glycinergic synaptic signaling (23). In contrast, our results strongly
354 suggest that an agonistic action on GlyT1 could be a key component for GE treatment. Here we
355 propose that agonizing GlyT1 activity may have a broader action in the brain by
356 counterbalancing hyperglycinemia both at the glycinergic and glutamatergic/NMDA synapse.
357 However, the attenuation of glycine signaling in the brain can have important side effects that
358 have to be considered, as exemplified by the poisoning effect of strychnine, a potent glycine
359 receptor antagonist (24). As a result, such a therapeutic strategy would require the design and
360 development of GlyT1 agonists with varying potency, whose activity could be efficiently
361 adjusted to each GE patients.

362 At this juncture, our GLDC-KO zebrafish model could be of prime interest for drug-
363 screen purposes. Indeed, we showed that motor phenotypes relevant to the disease can be
364 accurately observed and quantified as early as 20 hours post fertilization. Moreover, we used
365 an automated quantification of coiling behavior that would allow for high-throughput
366 phenotyping. As a result, our zebrafish line and our phenotyping assay could serve as an initial
367 screening tool for testing the effects of newly designed drugs, such as GlyT1 agonists, that could
368 then be tested in mammalian models. Of note that many CNS-related disorders have been

successfully modeled in the past such as Amyotrophic Lateral Sclerosis and Spinal Muscular Atrophy, epilepsy, and autism (25-29).

Our work shed new light on another facet of GE as our metabolomics analysis unraveled unexpected changes in other metabolites than glycine itself. Interestingly, some of the amino acids that are increased in *gldc -/-* larvae (i.e. leucine and valine) are associated with another metabolic disease, maple syrup urine disease (MSUD). In patients suffering from MSUD, the metabolism of branched-chain amino acids (BCAA), such as leucine, isoleucine, and valine, is impaired due to mutations in subunits of the branched-chain α-keto acids dehydrogenase (BCKD). The levels of BCAA are thus increased in the urine, leading to a peculiar maple syrup smell. Remarkably, MSUD patients show some common symptoms to GE patients, such as hypotonia, seizures and the only efficient treatment is a BCAA-free diet. In order to test the effect of an excess of valine or leucine on the motor phenotype of zebrafish, we treated WT embryos with these single amino-acids or in combination and found that they induce a reduction of the coiling and swimming activity as strong as when treated with glycine (data not shown). These results therefore suggest that valine and leucine may play a role in GE pathogenesis. However, GE patients' blood and urine samples are rarely tested for other amino-acid levels, thus limiting our interpretation.

We believe these findings should instigate more profound metabolic testing of human patients, such as dosage of BCAAs, lactate in the blood and/or urine, and glutamate and GABA in the CSF. This could allow identifying putative defects in other amino acid metabolism, and therefore opening new therapeutic strategies that may not have been considered, such as a BCAA-free diet. However, the fact that all BCAAs are not found elevated in gldc-/- fish (such as

391 isoleucine) suggests that this effect could not be generalized to all BCAAs but may rely on more
392 specific mechanisms targeting leucine and valine. In this regard, a potential molecular link
393 between GE and MSUD might involve the dihyrolipoamide dehydrogenase (DLD) subunit, which
394 is part of both the GCS and the BCKD complexes. In human, DLD-deficiency leads to various
395 symptoms, such as severe seizures and encephalopathy, muscle weakness, accumulation of
396 pyruvate, lactate, BCAA and the related metabolites (30, 31). Interestingly, we observed
397 common phenotypes such as hypotonia, increased BCAA (e.g. valine, leucine) as well as lactate
398 in *gldc -/-* mutants, suggesting that *gldc* knockout might affect the activity of other metabolic
399 complexes and therefore induce a broad metabolic defect. Our metabolomic assay also showed
400 an increase of arginine in gldc-/- larvae. It is worth noting that as a precursor of nitric oxide and
401 polyamine, L-arginine regulates basic physiological functions and it has been shown to be a
402 player in age-related degenerative diseases such as Alzheimer's disease(32).
403 Previous studies from Greene et al. showed an imbalance in folate-related metabolites
404 in *Gldc* knock-out mice(7, 16). However, we did not detect any anomaly in the levels of FOCM
405 compounds in *gldc -/-* larvae (7). One possible explanation for this is that serine degradation,
406 another source of one-carbon units to the FOCM, could compensate for the loss of carbon-units
407 from glycine degradation(33), in addition, to the possibility that such an effect would be cell-
408 type or stage-specific (see above). Moreover, the proportion of 1C carrying folates was found
409 to be markedly lower in fish larvae than in mammalian tissue (pre- and post-natal). Thus, THF
410 represents approximately 60% of total folate, perhaps suggesting a lesser requirement for 1C-
411 carrying folates in zebrafish larva than in mammalian cells and tissues (mouse and human) or
412 bacteria in which 5-methyl THF or formyl-THF are predominant(15). Thus, these results suggest

that FOCM disturbances may not be directly involved in the motor dysfunction associated with GE, but rather specifically in structural malformations such as neural tube defects.

Altogether, the present work confirmed the central role played by the hyperglycinemia in motor dysfunction associated with GE, but also unraveled an unexpected broader metabolic disturbance that could also be essential in GE pathogenesis. Both aspects of the disease should be considered in the design of new therapeutic strategies aiming at saving GE neonates as well as ameliorating surviving GE patients' quality of life. Among these strategies, our findings suggest that the development of glycine transporter 1 agonists would be a putative promising avenue, as well as BCAAs-free diet.

Methods

Genetic testing and glycine titration in patients

Blood sample from patients have been tested for NKH by PCR amplification and direct DNA sequencing in both directions of the 9 exons of *AMT* gene and 25 exons of *GLDC* gene as well as the intron/exon borders. All the genetic testing have been performed at Denver Genetic Laboratories.

Fish Husbandry and fish lines

Wild-type zebrafish (*Danio rerio*) were reared at 28.5°C, kept under a 12-hour dark, 12-hour light cycle and staged as described previously (34). They were bred according to standard procedures (35). All experiments were performed in compliance with the guidelines of the

Canadian Council for Animal Care and conducted at the Research Center of the University of Montreal Hospital Center (CRCHUM). The dlx5-6:GFP, islet1:GFP and vglut2a:RFP transgenic lines are gifts from Marc Ekker and Shin-ichi Higashijima respectively (21, 36).

Whole mount *in situ* hybridization and probe cloning

A Specific *gldc* probe corresponding to the 5' part of the coding sequence and first exon (951bp amplified with the following primers: Forward-gaaggacctttgtgagattacgg; Reverse-taatgcaggccagtgagtgag) was cloned within the pCS2+ vector using TOPO TA cloning kit (Invitrogen). Whole-mount *in situ* hybridization of zebrafish embryos was performed as described by (37).

sgRNA and cas9 preparation and microinjection

The following gRNA sequence targeting the fourth exon of the *gldc* gene was designed using the online tool CRISPRscan ((PAM site is indicated in brackets): gggacacctcgggctggta(cgg). Synthesis of gRNA and Cas9 mRNA was performed as described by (12). Wild-type embryos were collected for microinjection. A 1nL drop of a mix of 100 ng/µL of Cas9 mRNA and 30 ng/L of gRNA was injected into one-cell stage embryos.

High-resolution melting (HRM)

Primers were designed using the Universal Probe Library Assay Design Center (Roche). Forward: TTCAGTGAGTATTTGTGTTCTCTACAGG; Reverse: TGGTCTGATAGTTGAGTAAGCTCTCC. The PCR reactions was performed as described by (12).

Coiling analysis and swim tracking

20hpf embryos were embedded in low melting agarose and covered with water, their movements inside the chorion were recorded using a camera for 20 minutes. The Danioscope software (Noldus) was then used to quantify the number of bursts over time. At 7 dpf, larvae were transferred individually into a 96-well plate and swim distance was recorded using Basler GenIcam camera and DanioVision recording chamber (Noldus). Analysis was performed using the Ethovision XT 12 software (Noldus) to quantify the distance swam.

Hypotonia and swim balance tests

One gldc -/- mutant and one sibling 7 dpf larva were placed in the center of a water-filled petri dish and a water current was manually applied. For the swimming balance test, a heat map tracking the movement of the larvae using the Noldus Danio Vision software was generated over 10 minutes.

Mass spectrometry liquid chromatography

Analysis of multiple folates was performed by UPLC-MS/MS as described previously (16). Amino acids were detected and quantified by LC-MS/MS as previously described (38, 39). Processing of the chromatograms obtained by LC-MSMS was done using TargetLynx (Waters), including peak detection, peak integration and concentration estimation based on calibration curves. For statistical analyses, Student's T-test was used. Significance testing and graphing was

performed with GraphPad Prism 7 software. Analysis of the neurotransmitter and lactate was performed as described by (40). The extraction details are available upon request.

Transcriptomic assay, differential expression assay and pathway analysis

Total RNA was extracted from 7 dpf *gldc -/-* and *+/+* larvae using picopure RNA extraction kit (Thermo Fisher Scientific) following the manufacturer's standard protocol. Quality of total RNA was assessed with the BioAnalyzer Nano (Agilent) and all samples had a RIN above 9.

Library preparation was done as described by (41). Sequencing was performed with the Illumina NextSeq500 using the SBS Reagent Kit v3 (100 cycles, paired-end) with 1.6 nM of the pooled library. Cluster density was targeted at around 800k clusters/mm^2. Between 73 and 98 million reads were generated for each sample. Library preparation and sequencing was done at the Institute for Research in Immunology and Cancer's Platform (University of Montreal). About 95% of high quality reads were mapped onto the zv9 version of the zebrafish genome (ensemble release 77) using TopHat version 2.0.10.

Differential gene expression analysis was assessed by DeSeq2 package using R software. Differential gene expression was filtered on a False Discovery Rate (or adjusted p value > 0.05). Pathway analysis was performed using DAVID bioinformatics resources (42). The list of differentially expressed genes was uploaded onto DAVID analysis wizard and a list of all expressed genes found in our dataset was used as a background for gene enrichment analysis.

Immunohistochemistry and pH3 and pav7 quantification

Gldc -/- and *+/+* embryos were anaesthetized in 0.2% tricaine, fixed with 4% paraformaldehyde for 1h30 at room temperature (or in Dent's overnight at 4ºC for pH3 IHC). Immunohistochemistry was performed as previously described (43) with anti Ac-Tub (1:1000, T6793, sigma), anti-pH3 (polyclonal, 1:500, 06-570, millipore), anti-TH (1:400, mab318, millipore), anti vGluT1 (1:500), or anti-pav7 (1:1000, both gifts of Masahiko Hibi). Quantification of Pav7- and pH3-positive cells was done blindly by using the count tool on Photoshop.

Drug treatments

All drugs were obtained through Sigma. The drug solutions were prepared as follows: 10mM stock solution of strychnine (S0532) was prepared by dissolving 33.4mg of powder in 10mL of water; 10mM stock solution of Dextromethorphan (D9684) was prepared by dissolving 37mg of powder in 10mL of water. The stock solution was dissolved in fish water to reach the final concentration. Embryos and larvae were individualized in glass beaker in a total volume of 50mL and were incubated overnight in a lightproof box at 28.5ºC.

Glycine Transporter 1 cloning and mRNA in vitro synthesis

Full-length cDNA of GlyT1 was cloned from 24 hpf total RNAs using the following primers: Forward : ATGAACAGCAGAAAGAATGGAGCA; Reverse : CTATGCGCTGGGTGTGGG. The PCR product was cloned within the pCS2+ vector using TOPO TA cloning kit (Invitrogen). After sequencing, the corresponding mRNA was transcribed *in vitro* using SP6 RNA polymerase.

Statistics

Statistical analysis for comparing two groups were performed using a t-test. When comparing more than two groups, the statistical analysis performed corrected for multiple comparisons and also for repeated measures when comparing multiple measurements between groups using a Bonferroni correction for multiple comparisons. Raw results are displayed with box and whiskers showing the min and max values as well as the median value (line).

Study approval

Genetic testing were performed under written consent from the patients. All experiments were performed in compliance with the guidelines of the Canadian Council for Animal Care and conducted at the Research Center of the University of Montreal Hospital Center (CRCHUM). The vertebrate animal welfare assurance from the Institutional Animal Care and Use Committee (IACUC) for the use of adult zebrafish has been approved on 2015/08/31.

Author contributions

RR and ES designed and performed all the zebrafish research experiments as well as wrote the manuscript. IP, K-IL, NP and NG performed the mass spectrometry analysis. ML performed the molecular biology research. KS and LAS performed the clinical study. PD, RR and ES reviewed the manuscript.

Acknowledgments

We thank Marina Drits of the CRCHUM zebrafish platform, Florent Guilloteau and Patrick Gendron from the IRIC genomic platform. This work was funded by The Grand Défi Pierre

Lavoie, The Savoy Foundation, the Fonds de Recherche Québec Santé (FRQS), the Rare Disease Model and Mechanism network, FRQS-affiliated GRSNC (Groupe de Recherche sur le Système Nerveux Central), the Québec MEESR (Ministère de l'Éducation, de l'Enseignement Supérieur et de Recherche) and the CRCHUM. NG and KL were funded by the MRC (N003713) and Joseph's Goal.

References

1. Dulac O, and Rolland M-O. Nonketotic Hyperglycinaemia (Glycine Encephalopathy). 2012:349-56.
2. Baker PR, 2nd, Friederich MW, Swanson MA, Shaikh T, Bhattacharya K, Scharer GH, Aicher J, Creadon-Swindell G, Geiger E, MacLean KN, et al. Variant non ketotic hyperglycinemia is caused by mutations in LIAS, BOLA3 and the novel gene GLRX5. *Brain.* 2014;137(Pt 2):366-79.
3. Korman SH, and Gutman A. Pitfalls in the diagnosis of glycine encephalopathy (non-ketotic hyperglycinemia). *Developmental medicine and child neurology.* 2002;44(10):712-20.
4. Hennermann JB, Berger J-M, Grieben U, Scharer G, and Van Hove JL. Prediction of long-term outcome in glycine encephalopathy: a clinical survey. *Journal of inherited metabolic disease.* 2012;35(2):253-61.
5. Coughlin CR, 2nd, Swanson MA, Kronquist K, Acquaviva C, Hutchin T, Rodriguez-Pombo P, Vaisanen ML, Spector E, Creadon-Swindell G, Bras-Goldberg AM, et al. The genetic basis of classic nonketotic hyperglycinemia due to mutations in GLDC and AMT. *Genet Med.* 2017;19(1):104-11.
6. Bjoraker KJ, Swanson MA, Coughlin CR, 2nd, Christodoulou J, Tan ES, Fergeson M, Dyack S, Ahmad A, Friederich MW, Spector EB, et al. Neurodevelopmental Outcome and Treatment Efficacy of Benzoate and Dextromethorphan in Siblings with Attenuated Nonketotic Hyperglycinemia. *J Pediatr.* 2016;170(234-9.
7. Pai YJ, Leung KY, Savery D, Hutchin T, Prunty H, Heales S, Brosnan ME, Brosnan JT, Copp AJ, and Greene ND. Glycine decarboxylase deficiency causes neural tube defects and features of non-ketotic hyperglycinemia in mice. *Nat Commun.* 2015;6(6388.
8. Kojima-Ishii K, Kure S, Ichinohe A, Shinka T, Narisawa A, Komatsuzaki S, Kanno J, Kamada F, Aoki Y, and Yokoyama H. Model mice for mild-form glycine encephalopathy: behavioral and biochemical characterizations and efficacy of antagonists for the glycine binding site of N-methyl D-aspartate receptor. *Pediatric research.* 2008;64(3):228.

9. Cui WW, Low SE, Hirata H, Saint-Amant L, Geisler R, Hume RI, and Kuwada JY. The zebrafish shocked gene encodes a glycine transporter and is essential for the function of early neural circuits in the CNS. *J Neurosci.* 2005;25(28):6610-20.
10. Swanson MA, Coughlin CR, Jr., and Van Hove JL. Corrigendum: Swanson MA, Coughlin CR Jr, Scharer GH, et al: Biochemical and molecular predictors for prognosis in nonketotic hyperglycinemia. Ann Neurol 2015;78:606-618. *Ann Neurol.* 2016;79(3):505.
11. Swanson MA, Coughlin CR, Jr., Scharer GH, Szerlong HJ, Bjoraker KJ, Spector EB, Creadon-Swindell G, Mahieu V, Matthijs G, Hennermann JB, et al. Biochemical and molecular predictors for prognosis in nonketotic hyperglycinemia. *Ann Neurol.* 2015;78(4):606-18.
12. Samarut E, Lissouba A, and Drapeau P. A simplified method for identifying early CRISPR-induced indels in zebrafish embryos using High Resolution Melting analysis. *BMC Genomics.* 2016;17(547.
13. Flusser H, Korman SH, Sato K, Matsubara Y, Galil A, and Kure S. Mild glycine encephalopathy (NKH) in a large kindred due to a silent exonic GLDC splice mutation. *Neurology.* 2005;64(8):1426-30.
14. Saint-Amant L, and Drapeau P. Time course of the development of motor behaviors in the zebrafish embryo. *Journal of neurobiology.* 1998;37(4):622-32.
15. Leung KY, De Castro SC, Cabreiro F, Gustavsson P, Copp AJ, and Greene ND. Folate metabolite profiling of different cell types and embryos suggests variation in folate one-carbon metabolism, including developmental changes in human embryonic brain. *Mol Cell Biochem.* 2013;378(1-2):229-36.
16. Leung K-Y, Pai YJ, Chen Q, Santos C, Calvani E, Sudiwala S, Savery D, Ralser M, Gross SS, and Copp AJ. Partitioning of One-Carbon Units in Folate and Methionine Metabolism Is Essential for Neural Tube Closure. *Cell reports.* 2017;21(7):1795-808.
17. Applegarth DA, and Toone JR. Nonketotic hyperglycinemia (glycine encephalopathy): laboratory diagnosis. *Mol Genet Metab.* 2001;74(1-2):139-46.
18. Hutchesson A, Preece MA, Gray G, and Green A. Measurement of lactate in cerebrospinal fluid in investigation of inherited metabolic disease. *Clinical Chemistry.* 1997;43(1):158-61.
19. Viola A, Chabrol B, Nicoli F, Confort-Gouny S, Viout P, and Cozzone PJ. Magnetic resonance spectroscopy study of glycine pathways in nonketotic hyperglycinemia. *Pediatric research.* 2002;52(2):292.
20. Kleta R, Romeo E, Ristic Z, Ohura T, Stuart C, Arcos-Burgos M, Dave MH, Wagner CA, Camargo SR, and Inoue S. Mutations in SLC6A19, encoding B 0 AT1, cause Hartnup disorder. *Nature genetics.* 2004;36(9):999.
21. Yu M, Xi Y, Pollack J, Debiais-Thibaud M, MacDonald RB, and Ekker M. Activity of dlx5a/dlx6a regulatory elements during zebrafish GABAergic neuron development. *International journal of developmental neuroscience.* 2011;29(7):681-91.
22. Kimura Y, Hisano Y, Kawahara A, and Higashijima S-i. Efficient generation of knock-in transgenic zebrafish carrying reporter/driver genes by CRISPR/Cas9-mediated genome engineering. *Scientific reports.* 2014;4(6545.

23. Tsai G, Lane H-Y, Yang P, Chong M-Y, and Lange N. Glycine transporter I inhibitor, N-methylglycine (sarcosine), added to antipsychotics for the treatment of schizophrenia. *Biological psychiatry.* 2004;55(5):452-6.
24. Boyd RE, Brennan PT, Deng J-F, Rochester DF, and Spyker DA. Strychnine poisoning: recovery from profound lactic acidosis, hyperthermia, and rhabdomyolysis. *The American journal of medicine.* 1983;74(3):507-12.
25. Schmid B, Hruscha A, Hogl S, Banzhaf-Strathmann J, Strecker K, van der Zee J, Teucke M, Eimer S, Hegermann J, Kittelmann M, et al. Loss of ALS-associated TDP-43 in zebrafish causes muscle degeneration, vascular dysfunction, and reduced motor neuron axon outgrowth. *Proceedings of the National Academy of Sciences.* 2013;110(13):4986-91.
26. McGown A, McDearmid JR, Panagiotaki N, Tong H, Al Mashhadi S, Redhead N, Lyon AN, Beattie CE, Shaw PJ, and Ramesh TM. Early interneuron dysfunction in ALS: insights from a mutant sod1 zebrafish model. *Annals of neurology.* 2013;73(2):246-58.
27. Oprea GE, Kröber S, McWhorter ML, Rossoll W, Müller S, Krawczak M, Bassell GJ, Beattie CE, and Wirth B. Plastin 3 is a protective modifier of autosomal recessive spinal muscular atrophy. *Science.* 2008;320(5875):524-7.
28. Baraban SC, Dinday MT, and Hortopan GA. Drug screening in Scn1a zebrafish mutant identifies clemizole as a potential Dravet syndrome treatment. *Nature communications.* 2013;4(2410.
29. Elsen GE, Choi LY, Prince VE, and Ho RK. The autism susceptibility gene met regulates zebrafish cerebellar development and facial motor neuron migration. *Developmental biology.* 2009;335(1):78-92.
30. Quintana E, Pineda M, Font A, Vilaseca MA, Tort F, Ribes A, and Briones P. Dihydrolipoamide dehydrogenase (DLD) deficiency in a Spanish patient with myopathic presentation due to a new mutation in the interface domain. *Journal of Inherited Metabolic Disease.* 2010;33(3):315-9.
31. Brassier A, Ottolenghi C, Boutron A, Bertrand A-M, Valmary-Degano S, Cervoni J-P, Chrétien D, Arnoux J-B, Hubert L, and Rabier D. Dihydrolipoamide dehydrogenase deficiency: a still overlooked cause of recurrent acute liver failure and Reye-like syndrome. *Molecular genetics and metabolism.* 2013;109(1):28-32.
32. Yi J, Horky LL, Friedlich AL, Shi Y, Rogers JT, and Huang X. L-arginine and Alzheimer's disease. *Int J Clin Exp Pathol.* 2009;2(3):211-38.
33. Locasale JW. Serine, glycine and one-carbon units: cancer metabolism in full circle. *Nat Rev Cancer.* 2013;13(8):572-83.
34. Kimmel CB, Ballard WW, Kimmel SR, Ullmann B, and Schilling TF. Stages of embryonic development of the zebrafish. *Dev Dyn.* 1995;203(3):253-310.
35. Westerfield M. *The Zebrafish Book: A Guide for the Laboratory Use of Zebrafish (Danio rerio).* Institute of Neuro Science; 1995.
36. Higashijima S-i, Hotta Y, and Okamoto H. Visualization of cranial motor neurons in live transgenic zebrafish expressing green fluorescent protein under the control of the islet-1 promoter/enhancer. *Journal of Neuroscience.* 2000;20(1):206-18.
37. Thisse C, and Thisse B. High-resolution in situ hybridization to whole-mount zebrafish embryos. *Nat Protoc.* 2008;3(1):59-69.

38. Pena IA, Roussel Y, Daniel K, Mongeon K, Johnstone D, Mendes HW, Bosma M, Saxena V, Lepage N, and Chakraborty P. Pyridoxine-dependent epilepsy in zebrafish caused by Aldh7a1 deficiency. *Genetics.* 2017;207(4):1501-18.
39. Waterval WH, Scheijen JL, Ortmans-Ploemen MM, Habets-van der Poel CD, and Bierau J. Quantitative UPLC-MS/MS analysis of underivatised amino acids in body fluids is a reliable tool for the diagnosis and follow-up of patients with inborn errors of metabolism. *Clinica chimica acta.* 2009;407(1-2):36-42.
40. Wojnicz A, Ortiz JA, Casas AI, Freitas AE, López MG, and Ruiz-Nuno A. Simultaneous determination of 8 neurotransmitters and their metabolite levels in rat brain using liquid chromatography in tandem with mass spectrometry: Application to the murine Nrf2 model of depression. *Clinica Chimica Acta.* 2016;453(174-81.
41. Swaminathan A, Hassan-Abdi R, Renault S, Siekierska A, Riche R, Liao M, de Witte PAM, Yanicostas C, Soussi-Yanicostas N, Drapeau P, et al. Non-canonical mTOR-Independent Role of DEPDC5 in Regulating GABAergic Network Development. *Curr Biol.* 2018.
42. Huang da W, Sherman BT, and Lempicki RA. Systematic and integrative analysis of large gene lists using DAVID bioinformatics resources. *Nature Protocols.* 2009;4(1):44-57.
43. Puverel S, Nakatani H, Parras C, and Soussi-Yanicostas N. Prokineticin receptor 2 expression identifies migrating neuroblasts and their subventricular zone transient-amplifying progenitors in adult mice. *J Comp Neurol.* 2009;512(2):232-42.

Figure and Figure Legends

A

	Patient 1	Patient 2
Onset	*Newborn (day 4)*	*Adult (50 y-o)*
Gene	*GLDC*	*GLDC*
Allele 1	*c.1153 C>T (p.Q385X)*	*c.1054delA (p.T352fster65)*
Allele 2	*c.941 ins16nt fs*	*c.1705C>T(p.A569T)*
First plasma glycine level	*125 umol/dL (0-57)*	*75 umol/dL (13-50)*
CSF glycine level	*33.8 umol/dL (0.2-2.0)*	
Ratio plasma to CSF level	*0.27 (abnormal >0.08)*	

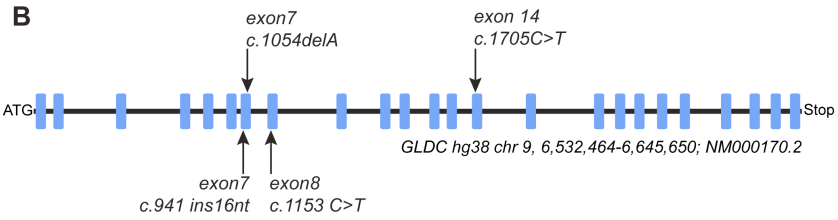

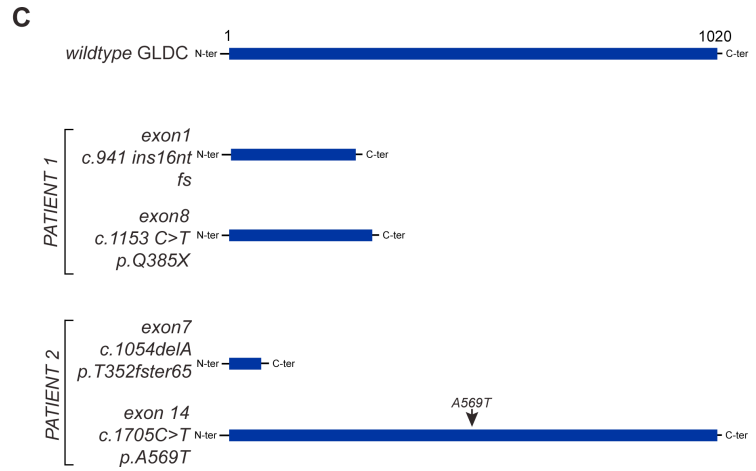

Riché et al., Figure 1

Figure 1: GLDC mutations associated with lethal or severe glycine encephalopathy. A. Genetic and molecular testing of the patients performed at the Denver Genetic Laboratories showing the mutation found in *GLDC* as well as plasma and cerebrospinal fluid (CSF) glycine level. B. The genetic position of each mutation is indicated on the scheme depicting the 25 exons of the *GLDC* gene. C. Consequences of the mutations on the expected GLDC protein size.

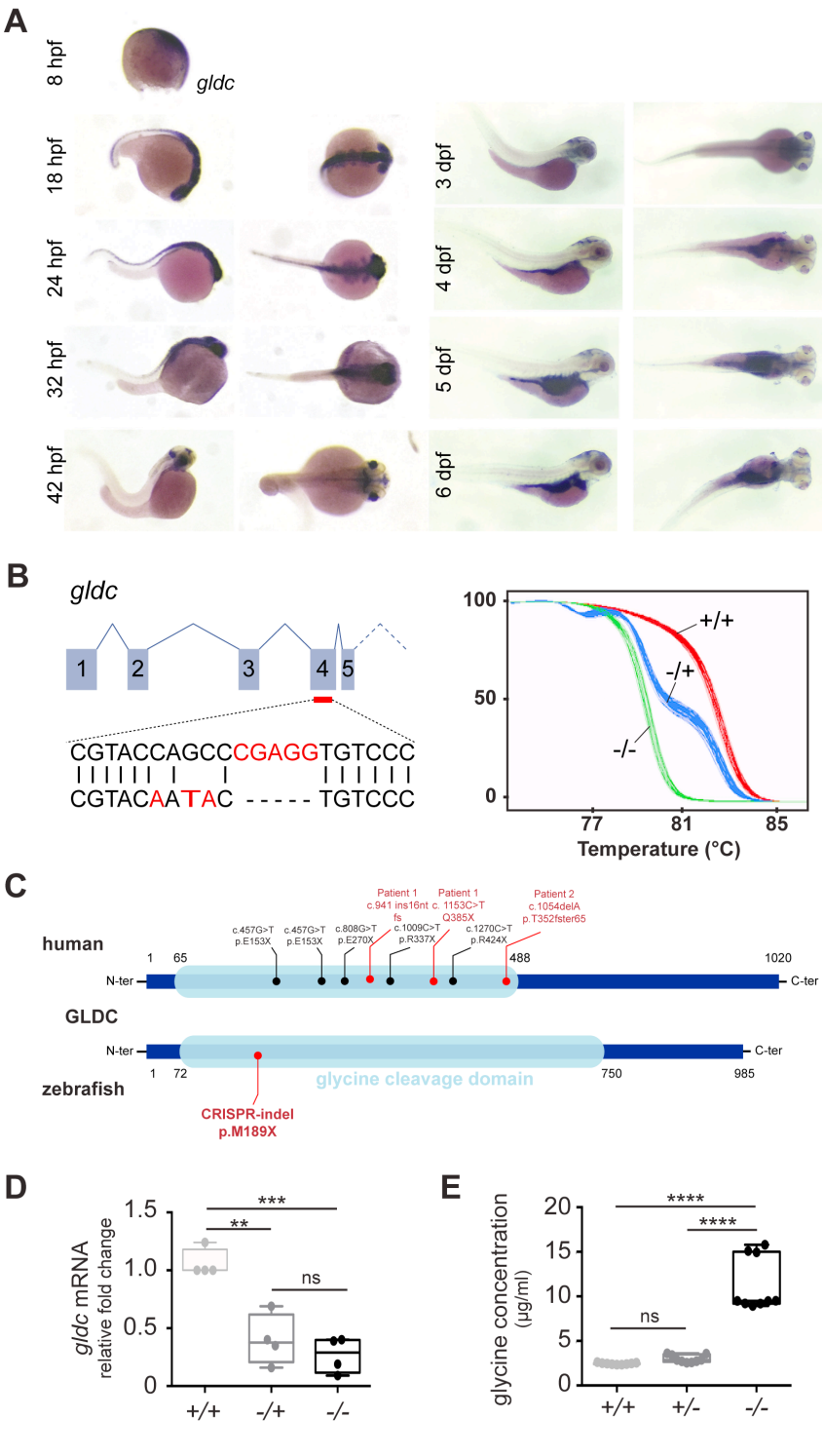

Riché et al., Figure 2

692

693 **Figure 2: Zebrafish *gldc* is expressed in the central nervous system and its loss-of-function**

694 **induces glycine accumulation.** A. In situ hybridization of *gldc* transcript at 8, 18, 24, 32, and 42

hours post fertilization (hpf) showing the expression in the brain and spinal cord as well as in the intestine at later stages. B. CRISPR/CAS9 mutagenesis targeting the 4th exon of *gldc* led to substitution of 2 nucleotides and deletion of 5 nucleotides. These DNA mutations in *gldc -/-* induce a melting curve shift compared to *+/+* that allows for rapid genotyping. C. Scheme of several nonsense mutations identified in patients leading to insertion of stop codons in the glycine cleavage domain of the human GLDC protein. In red, the mutant variant of the glycine encephalopathy patient described here, and in red in the zebrafish GLDC protein, the location of the CRISPR mutation. D. RT-qPCR analysis of the *gldc* mRNA levels, reveals a significant decrease in *gldc -/+* and *-/-* compared to *+/+*, at 7 dpf (ANOVA, ***: < 0.0004; **: < 0.005, n>10, N=3). LC-MS dosage of glycine levels in whole 7 days post fertilization larvae reveals a significant increase in *gldc -/-*, but not *-/+*, compared to *+/+* (ANOVA, ****: <0.0001, n=3, N=3). Box and whiskers display min and max values and a line shows the median value. Each dot corresponds to an individual experiment (N) of at least 5 fish (n>5).

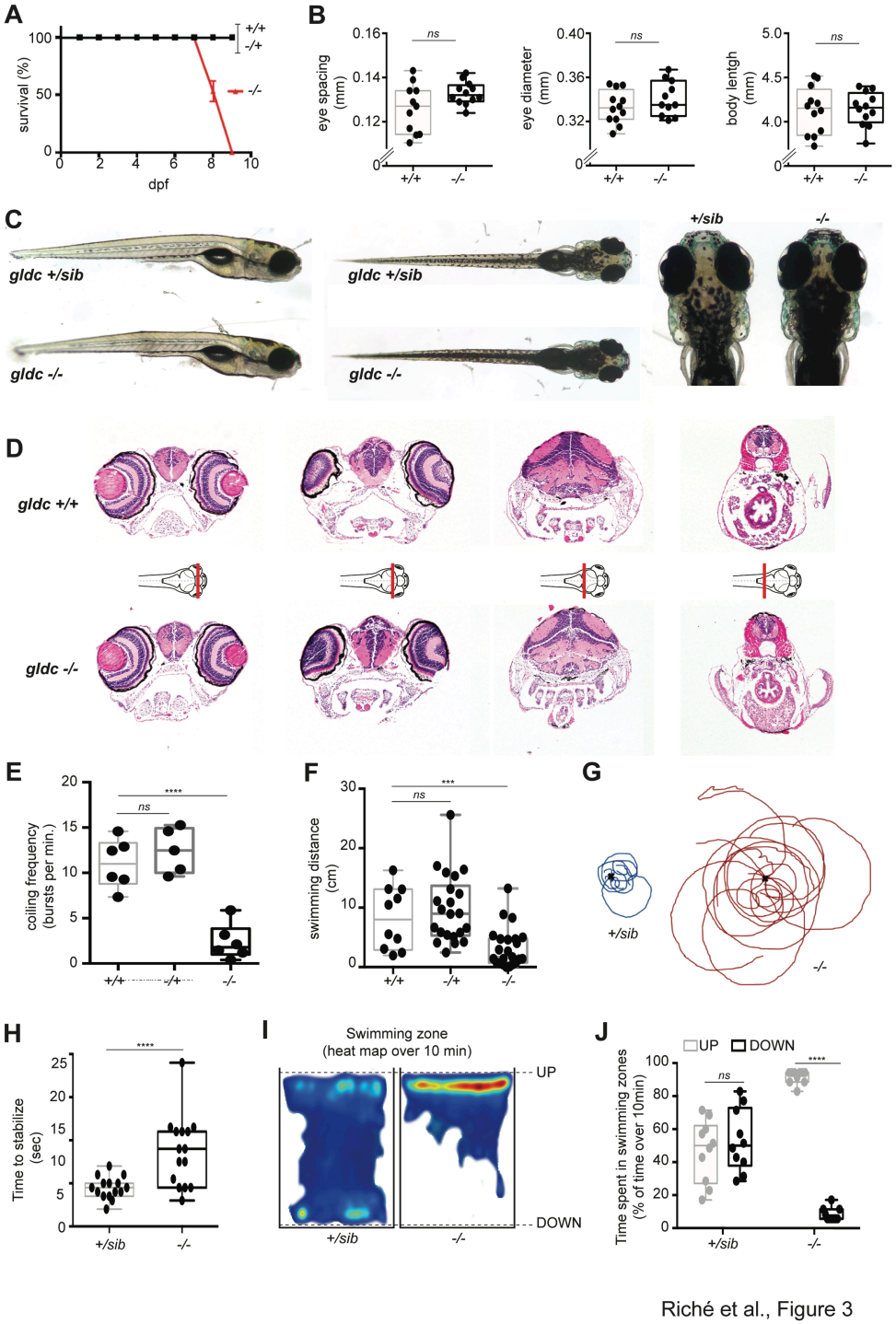

Riché et al., Figure 3

709

710 **Figure 3:** ***Gldc -/-*** **larvae die prematurely and depict disease-reminiscent motor phenotypes.** A.

711 *Gldc -/-* larvae die prematurely between 7 and 9 days post fertilization. B. The general

morphology of the fish is not affected as shown by the quantification of the eye spacing distance, eye diameter, and body length of *gldc -/-* compared to *+/+*. C. Although there is no obvious morphological defect in *gldc -/-* at 7 dpf, -/- larvae are distinguishable from their siblings thanks to their hyperpigmentation. D. Hematoxylin/Eosin staining performed on transverse sections from 7 dpf gldc+/+ and -/- larvae show no obvious difference of brain morphology. E. Analysis of the frequency of spontaneous coiling of the tail at 21 hours post fertilization, the earliest motor phenotype in zebrafish embryo, reveals a decrease of this behavior in *gldc -/-* larvae, compared to *+/+* (ANOVA p=0.0002). F. Analysis of the total distance swam over 1h at 7 days reveals a significant decrease of swimming in *gldc -/-* compared to *+/+* (ANOVA p=0.0077). G. Tracking of the position of gldc +/+ and -/- 7 days post-fertilization larvae from the center point after application of a water current show a balance problem of gldc-/- larvae. H. Indeed, *gldc -/-* larvae take significantly more time to stabilize their swimming after application of the water current compared to *gldc +/+* (t-test, p=0.0008). I. Heatmap tracking of the swimming zone of 7 dpf larvae over 10 min reveals that *gldc -/-* larvae are swimming only in the upper part of water, whereas *gldc +/+* swim in both upper and lower sections of the water. J. Quantification of the time spent in the upper versus lower swimming zone of the water reveals that *gldc -/-* spend significantly more time in the upper swimming zone compared to *+/+* (ANOVA, $p<0.0001$). Box and whiskers display min and max values and a line shows the median value. Each dot corresponds to an individual experiment (N) of at least 5 fish ($n>5$).

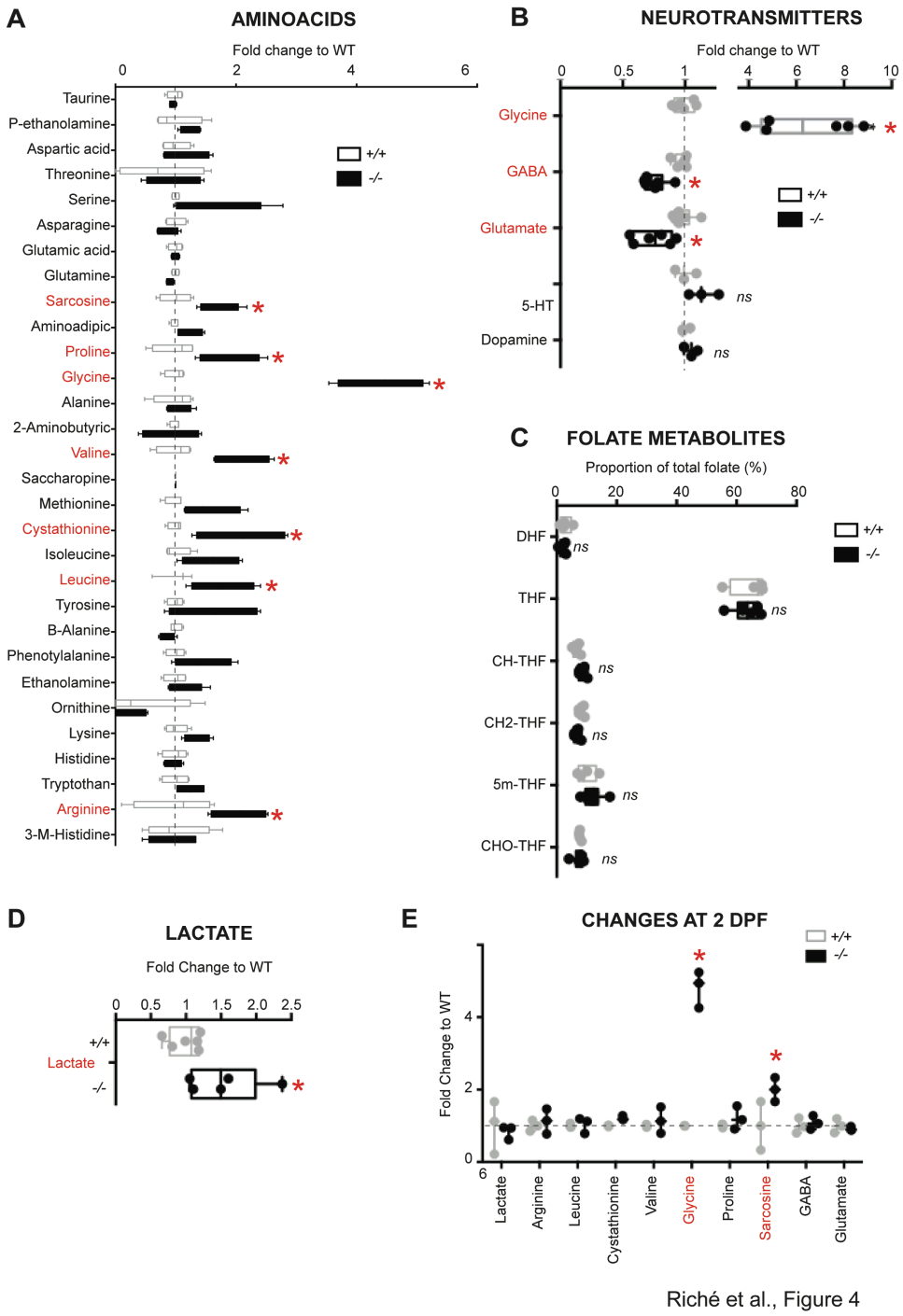

Riché et al., Figure 4

732

733 **Figure 4: Metabolomics analysis indicates broad metabolic perturbations in *gldc -/-* larvae.** A.

734 LC-MS analysis of the levels of the main proteogenic and non-proteogenic amino acids at 7 dpf

735 reveals a significant increase in sarcosine, proline, glycine, valine, cysthationine, leucine, and

arginine in gldc -/- compared to +/+ (t-test, respectively, p=0.035, p=0.0062, p<0.00001, p=0.0006, p=0.0006, p=0.029, and p=0.0006). B. LC-MS analysis of the main neurotransmitter at 7 dpf reveals a significant decrease in glutamate and GABA in *gldc -/-* compared to *+/+* (t-test, both p<0.00001). C. LC-MS analysis of folate compounds did not reveal any difference between *gldc -/-* and *+/+* at 7dpf. Box and whiskers display min and max values and a line shows the median value. Each dot corresponds to an individual experiment (N) of at least 3 fish (n>3).

A

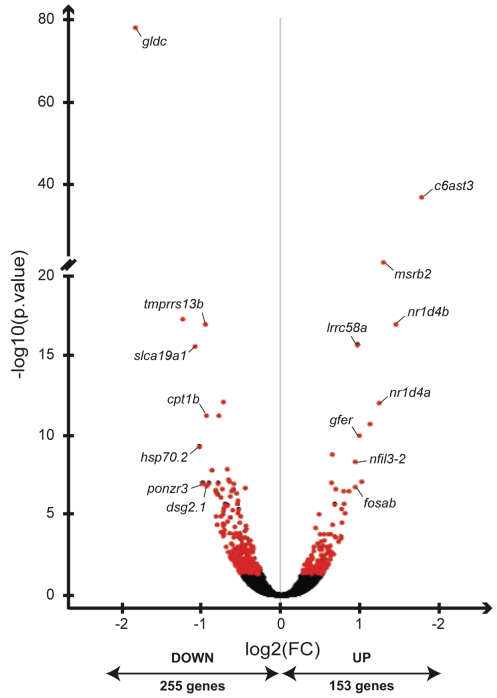

B

NEUROTRANSMISSION	Fold Change	p-value
slc6a9 (GlyT1)	-1.61	1.65e-08
METABOLISM		
msrb2 (methionine sufoxide reductase)	2.43	3.55e-22
***gfer* (growth factor)**	1.97	1.21e-10
lct (lactase)	1.55	2.11e-03
upp2 (uridine phosphorylase)	-1.73	7.07e-12
cpt1b (carnitine palmityltransferase)	-1.95	1.44e-17
slc6a19 (neutral amino acid transporter)	-2.14	3.61e-16
CELL CYCLE/GROWTH		
gadd45ba (growth arrest and DNA damage inducible)	1.72	3.39e-07
igflr1 (IGF-like family receptor)	1.69	4.48e-06
cdt1 (chromatin liscensing and DNA replication factor)	1.49	1.46e-02
mcm5 (minichromosome maintenance complex)	1.43	9.57e-04
ccne2 (cyclin E2)	1.43	4.60e-02
ONCOGENE/PROLIFERATION AND TUMOR SUPPRESSORS		
fos	1.90	1.89e-07
cuzd1 (CUB and zona pellucida-like domains 1)	1.80	3.71e-07
cdc7a (cell dicision cycle associated)	1.74	8.61e-06
egr4 (early growth response)	1.73	2.35e-06
mycb	1.55	1.03e-07
bcl6a (Chronic Lymphocytic Leukemia/lymphoma)	-1.45	6.44e-03
xiap (X-linked inhibitor of apoptosis)	-1.55	3.71e-07
foxq1a (forkhead box Q1a)	-1.65	4.19e-05
erb2b (estrogen recepotor)	-1.93	1.63e-07
EXTRA-CELLULAR MATRIX / CELL ADHESION		
itga6b (integrin alpha 6b)	-1.44	1.70e-04
itgb4 (integrin beta 4)	-1.50	6.18e-05
lama3 (laminin 3)	-1.70	1.29e-05

Riché et al., Figure 5

<u>Figure 5:</u> Transcriptomics analysis reveals differences in the expression of cell cycle, proliferation, and metabolism-related genes in the *gldc -/-* mutants. A. RNA sequencing analysis of 7 dpf larvae reveals that 408 genes are differentially expressed, with 255 up-regulated and 153 downregulated, in *gldc -/-* compared to *+/+*. B. Pathway analysis of the differentially regulated genes reveals that genes involved in metabolism, cell cycle/growth, oncogene/proliferation and tumor suppressor, extracellular matrix, and one in neurotransmission are mis-regulated in *gldc -/-* compared to *+/+*.

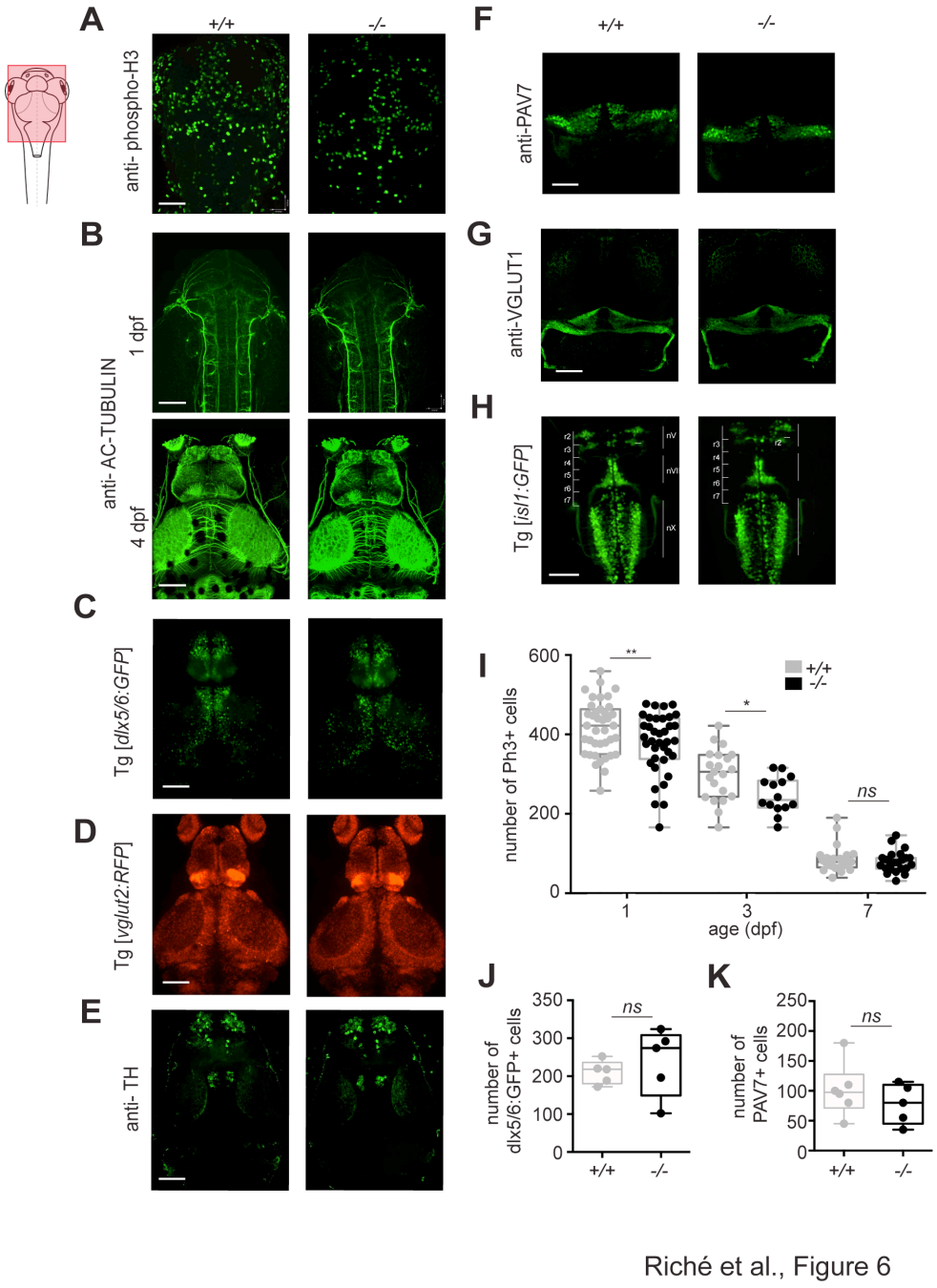

Riché et al., Figure 6

<u>Figure 6:</u> The main brain networks are not affected by gldc-KO despite a transient decrease of proliferation in *gldc -/-* brain. A. Immunohistochemistry against phospho-histone 3 (Ph3) labels proliferating cells on *gldc -/-* and *+/+* 3 dpf larvae. B. Immunohistochemistry against acetylated tubulin labelling axonal tracks did not reveal any gross morphological difference at 1 and 4 dpf

between *gldc -/-* and *+/+* larvae. C. The transgenic dlx5/6:GFP line was used to visualize GABAergic cells in *gldc -/-* and *+/+* 7 dpf larvae. D. Using the vGluT2:RFP transgenic line to label the glutamatergic network did not reveal any gross morphological difference between *gldc -/-* and *+/+* 7 dpf larvae. E. Immunohistochemistry against tyrosine hydroxylase labelling dopaminergic neurons did not reveal any gross morphological difference between *gldc -/-* and *+/+* at 5 dpf. F. Immunohistochemistry against paravalbumin 7 labels purkinje cells of the cerebellum on 5 dpf gldc -/- and +/+ larvae. G. Immunohistochemistry against vGluT1 labelling granule cells of the cerebellum did not reveal any gross morphological difference between 5dpf *gldc -/-* and *+/+* larvae. H. Using the islet1:GFP transgenic line to label the branchiomotor neuron network did not reveal any gross morphological difference between *gldc -/-* and *+/+* 3 dpf larvae. I. Quantification of the number of Ph3 positive cells revealed a significant decrease of proliferating cells in *gldc -/-* compared to *+/+* at 1 and 3 dpf, but not 7 dpf (t-test, respectively, p=0.0223 and p=0.014). J. Quantification of the number of dlx5/6:GFP positive cells did not reveal any difference between *gldc -/-* and *+/+*. K. Quantification of the number paravalbumin 7 positive cells did not reveal any difference between *gldc -/-* and *+/+*. Box and whiskers display min and max values and a line shows the median value. Each dot corresponds to an individual biological replicate (n>5).

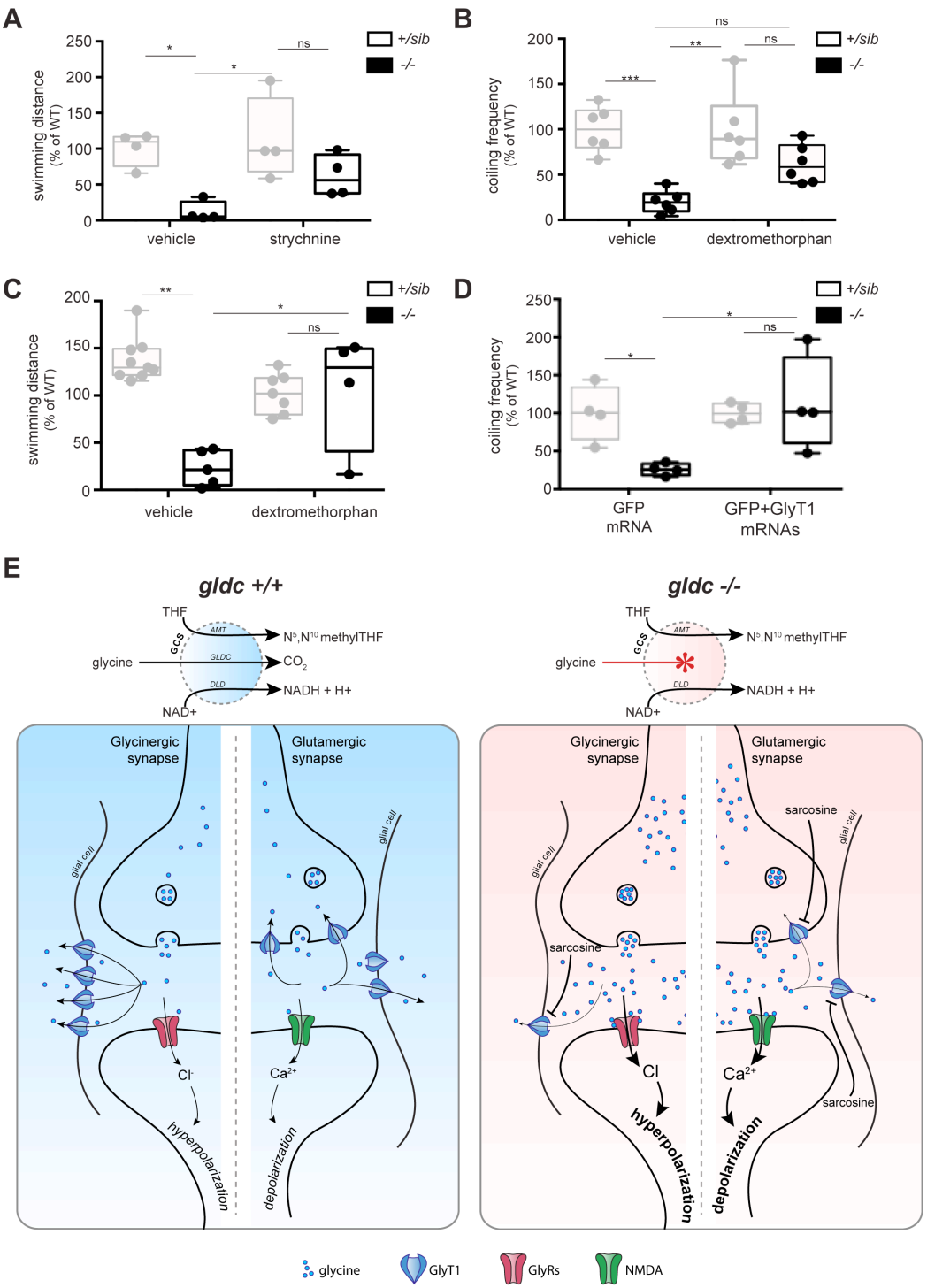

Riché et al., Figure 7

Figure 7: Genetically and pharmacologically counteracting the exacerbated hyperglycinemia at the synapse rescues the motor phenotype of *gldc -/-*. A. Overnight treatment with

778 strychnine 5uM significantly rescues the hypotonic swimming of gldc -/- (n=6) at 7 days
779 compared to vehicle treated gldc -/- (n=11) (p=0.0446; for vehicle treated -/- vs. sib/+,
780 p=0.0002). B. Overnight treatment with dextromethorphan 50uM decreases the hypotonic
781 coiling of gldc -/- (n=23) compared to vehicle treated gldc -/- embryos (n=27) at 21 hpf, (vehicle-
782 treated sib/+ vs. dextromethorphan-treated sib/+, p<0.0001; vehicle-treated sib/+ vs. -/-,
783 p=0.0013). C. Daily dextromethorphan 25uM treatment over 7 days significantly rescues the
784 hypotonic swimming of gldc -/- (n=4) at 7 days, compared to vehicle-treated gldc -/- larvae
785 (n=6) (p=0.0129; vehicle-treated sib/+ vs. -/-, p=0.0017). D. First-cell stage Glycine Transporter 1
786 (GlyT1) mRNA injection rescues the coiling defect of gldc-/- embryos at 21 hours post
787 fertilization compared to GFP injected gldc -/- (n>15, N=4) (p=0.0064; GFP-injected sib/+ vs. -/-,
788 p=0.015). E. Model representation of NMDA and glycine synapses of *gldc -/-* compared to *+/+.*
789 *Gldc -/-* have an exacerbated hyperglycinemia at these synapses due to a decrease in GlyT1 and
790 an increase in the levels of sarcosine. Box and whiskers display min and max values and a line
791 shows the median value. Each dot corresponds to an individual experiment (N) of at least 5 fish
792 (n>5).
793